Reflective Semiconductor Optical Amplifier Pulse Propagation Model

Michael J. Connelly, *Member, IEEE*

***Abstract*— A simple time-domain model for optical pulse propagation in a reflective semiconductor optical amplifier (RSOA) is described. The RSOA saturation energy, effective carrier lifetime, and spectral hole-burning parameters used in the model are determined using experimental measurements of the input and output pulse temporal profiles to the RSOA and least mean-square fitting. The model accurately predicts the propagation of 39.6 ps pulsewidth variable energy pulses in the RSOA. The model is used to predict the RSOA gain dynamics, spatial dependence of the pulse shape, and dynamic chirp.**

***Index Terms*— Pulse propagation modeling, reflective semiconductor optical amplifier (RSOA).**

I. Introduction

THE semiconductor optical amplifier (SOA), utilized as an active nonlinear optical medium, has demonstrated its feasibilities in all optical functional applications, such as optical switching and wavelength conversion. Reflective semiconductor optical amplifiers (RSOAs) utilize a high reflective coating on one facet and an anti-reflective coating on the other facet to produce a highly versatile gain medium. Although its waveguide structure is similar to a conventional SOA, RSOAs have a low noise figure and high optical gain at low drive currents. RSOAs have shown promise for applications in wavelength division multiplexed passive optical networks (PONs) and in fiber ring mode-locked lasers [1]–[3]. It is of interest to model the amplification of optical pulses in RSOAs. In this letter we use a simple bidirectional pulse propagation model to predict the propagation of 39.6 ps pulsewidth input pulses of in a tensile-strained RSOA [4], [5] and use least mean-square fitting to extract the RSOA saturation energy, effective lifetime and spectral hole burning parameter.

II. Model

The RSOA modeled has the same structure as the device in [4], [5], with a length L of 400 μm and a highly reflective coating applied to the rear facet. The model used is similar to the pulse propagation model described in [6], but uses actual RSOA device parameters obtained using the detailed model [5].

Manuscript received June 21, 2011; revised September 26, 2011; accepted October 16, 2011. Date of publication October 21, 2011; date of current version January 5, 2012. This work was supported in part by Science Foundation Ireland Investigator under Grant 09/IN.1/I2641.

The author is with the Department of Electronic and Computer Engineering, Optical Communications Research Group, University of Limerick, Limerick, Ireland (e-mail: michael.connelly@ul.ie).

Color versions of one or more of the figures in this letter are available online at http://ieeexplore.ieee.org.

Digital Object Identifier 10.1109/LPT.2011.2173184

In the slowly-varying envelope approximation, the forward and backward propagating envelopes $A^{\pm}$ of the optical field ($|A|^2$ is equal to the optical power) in the RSOA obey

$$\frac{\partial A^{\pm}}{\partial z} \pm v_g^{-1}\frac{\partial A^{\pm}}{\partial t} = \pm\frac{g}{2\left[1+\varepsilon\left(\left|A^{+}\right|^2+\left|A^{-}\right|^2\right)\right]} \times (1-j\,\alpha)\,A^{\pm} \tag{1}$$

where v_g is the group velocity and α the linewidth enhancement factor. The single-pass transit time L/v_g is 5.1 ps. The gain coefficient g rate-equation is

$$\frac{\partial g}{\partial t} = \frac{(g_0-g)}{\tau} - \frac{1}{E_{sat}}\frac{g\left(\left|A^{+}\right|^2+\left|A^{-}\right|^2\right)}{2\left[1+\varepsilon\left(\left|A^{+}\right|^2+\left|A^{-}\right|^2\right)\right]} \tag{2}$$

g_0 is the unsaturated gain coefficient, τ the effective carrier lifetime, E_{sat} the saturation energy and ε a spectral hole burning parameter. Assuming the RSOA has reflectivities of 0 and 1 at the input and reflective ends respectively the boundary conditions are $A^{+}(0,t) = \sqrt{P_{in}(t)}\exp[j\phi(t)]$ and $A^{-}(L,t) = A^{+}(L,t)$. $P_{in}(t)$ is the input pulse power and $\phi(t)$ is the pulse phase, which is equal to $2\pi\int_0^t \Delta\nu(t)\,dt$, where $\Delta\nu(t)$ is the pulse dynamic chirp and $t=0$ is the simulation start time. To obtain a stable numerical solution for (1), (2), we use the method of [6] whereby two independent space-time intervals are defined by

$$u = (T+z)/2 \quad v = (T-z)/2 \tag{3}$$

with reduced time $T = v_g t$ (units of distance). (3) is used to transform (1) to

$$\frac{\partial A^{+}}{\partial u} = \frac{g(z,t)}{2\left[1+\varepsilon\left(\left|A^{+}\right|^2+\left|A^{-}\right|^2\right)\right]}(1-j\alpha)A^{+} \tag{4}$$

$$\frac{\partial A^{-}}{\partial v} = \frac{g(z,t)}{2\left[1+\varepsilon\left(\left|A^{+}\right|^2+\left|A^{-}\right|^2\right)\right]}(1-j\alpha)A^{-}. \tag{5}$$

The derivatives in (2) and (4), (5) can be approximated by first-order finite differences to give

$$\begin{aligned} A^{+}(u+\Delta,v) &= A^{+}(u,v)+F_1(u,v)\Delta \\ A^{-}(u,v+\Delta) &= A^{-}(u,v)+F_2(u,v)\Delta \\ g(z,T+\Delta) &= g(z,T)+F_3(z,T)\Delta. \end{aligned} \tag{6}$$

The step size $\Delta = L/M$, where M is the number of spatial steps. Δ is also the step size of the reduced time. $F_{1,2,3}$ are the RHSs of (1), (2). The computation procedure is that if

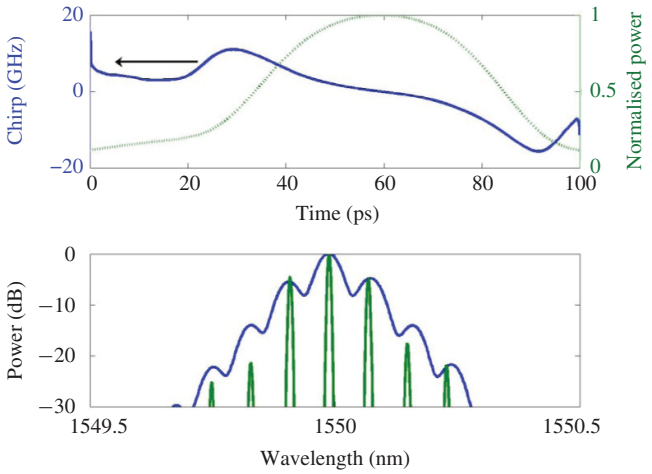

Fig. 1. Top: Input pulse power and chirp. Bottom: Pulse train spectrum.

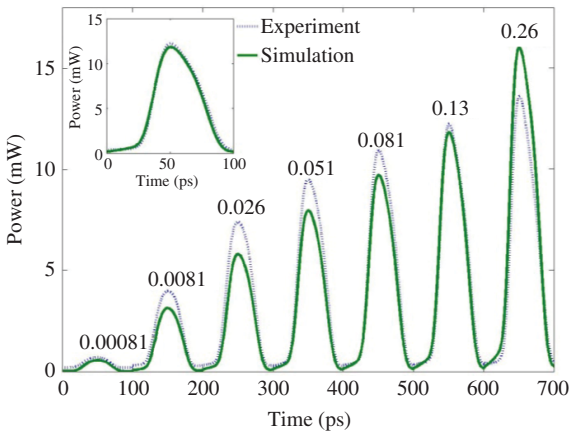

Fig. 2. Comparison between experimental and modelled output pulses for various input pulse energies (labelled in pJ). The pulses are shown on the same time axis for comparison. The inset shows a comparison between experiment and the model for an input pulse energy of 0.13 pJ.

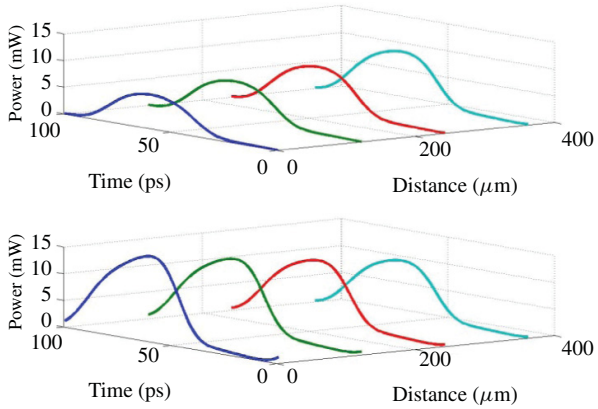

Fig. 3. Spatial evolution, at internals of 100 μm of a forward (top) and reflected (bottom) amplified pulse in the RSOA. The input pulse energy is 0.26 pJ. The distance is measured from the RSOA input.

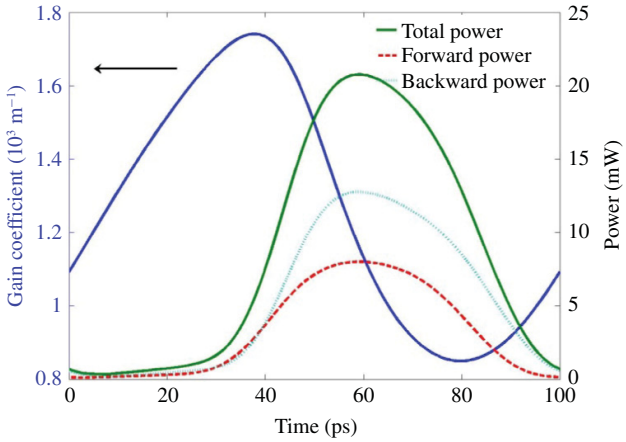

Fig. 4. Typical RSOA gain coefficient dynamics. The position is 200 μm and the input pulse energy is 0.26 pJ.

the state of the system is known at $T = n\Delta$, where n is an integer, then the state of the system for the internal spatial points $(m = 0 \ldots M)$, at $T = (n+1)\Delta$ is given by

$$\begin{aligned} A^+(m, N+1) &= A^+(m, N) + F_1(m-1, N)\Delta; \quad m \neq 0 \\ A^-(m, N+1) &= A^-(m+1, N) + F_2(m+1, N); \quad m \neq M \\ g(m, N+1) &= g(m, N) + F_3(m, N)\Delta \end{aligned} \tag{7}$$

subject to the boundary conditions given above. In the simulations we used $M = 100$, which corresponds to spatial and time step sizes of 4 μm and 0.051 ps respectively.

III. Experiment and Simulations

To apply the model to a real system, we experimentally determined the temporal power profile of amplified pulses from the RSOA when injected with a 10 GHz repetition rate stream of optical pulses with a pulsewidth of 39.6 ps at various pulse energies. The optical pulses were generated by modulating a 1550 nm laser using an electroabsorption modulator (EAM) driven by a 10 Gb/s clock signal from a pattern generator. The pulse train power and spectrum were measured using a 65 GHz optical bandwidth digital communications analyzer and a 0.06 nm resolution optical spectrum analyzer. The EAM had a chirp parameter of 0.85. The measured input pulse power profile, estimated chirp (determined using the chirp parameter and the pulse shape [7]) and pulse train spectrum are shown in Fig. 1. The measured pulses were used as the input to the RSOA model. The simulation time scale was 500 ps and the last pulse was used for comparison with experiment and parameter extraction. The linewidth enhancement factor used in the model was 1.7, which was determined using [8]. The SOA has a round-trip internal gain of 15 dB, which corresponds to $g_0 = 4.3 \times 10^3\,\mathrm{m}^{-1}$. The unknown parameters in the model are τ, E_{sat} and ε, which were determined using a least mean-squares fit (Levenberg-Marquardt algorithm) between the predicted and experimental output pulse power for input pulse energies of 0.00081, 0.0081, 0.026, 0.05, 0.08, 0.13, and 0.26 pJ. The parameter values obtained were $\tau = 132$ ps, $E_{sat} = 0.45$pJ, and $\varepsilon = 0.92\,\mathrm{W}^{-1}$. A comparison between the experimental output pulses and model predictions is shown in Fig. 2, showing good agreement between the model and simulations. The pulse peak gains are 9.7, 7.3, 4.9, 3.3, 2.2, 1.1 and -0.5 dB corresponding to the seven input pulse energies used. The modeled output

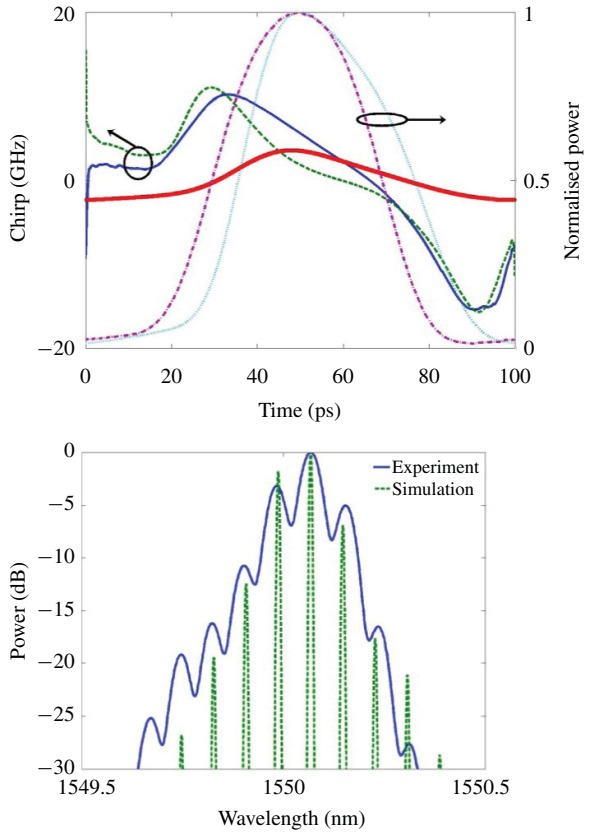

Fig. 5. Top: Modelled output chirp (solid line–output chirp; dashed line–input chirp; thick line–output chirp with unchirped input pulse; dotted line–output pulse; dashed–dotted line–output pulse). Bottom: Pulse train spectrum. The input pulse energy is 0.26 pJ. The modelled spectrum has a narrower spectral resolution than the measured spectrum.

pulsewidths increase from 39.7 ps to 41.9 ps, over this wide range of saturation levels, which are almost the same as the input pulsewidth. The model also predicts the increasing asymmetry of the amplified pulses with increasing saturation level. A typical predicted spatial evolution of the amplified pulse temporal power profile, in both propagation directions and gain coefficient dynamics are shown in Figs. 3 and 4. The gain and pulse dynamics are influenced by the transit time, which determines the time that pulses reflected from the end facet collide with the forward propagating pulses. This effect is not present in conventional SOAs. The model can be used to predict the amplified signal chirp and pulse train spectrum as shown in Fig. 5. The output pulse chirp profile is reasonably linear over the pulsewidth and thereby is amenable to dispersion compensation using a suitable length of dispersion compensating fiber or a chirped fiber Bragg grating. Fig. 5 also shows the modeled output pulse chirp for an unchirped input pulse. This chirp is also approximately linear and also amenable to dispersion compensation.

IV. Conclusion

A model for pulse propagation in RSOAs, which predicts the amplified pulse temporal and spectral characteristics, has been developed and experimentally verified. The model has potential applications in optimizing RSOAs and predicting the behavior of optical subsystems incorporating RSOAs, such as fiber ring lasers and PONs.

References

[1] E. Wong, K. L. Lee, and T. B. Anderson, "Directly modulated self-seeding reflective semiconductor optical amplifiers as colorless transmitters in wavelength division multiplexed passive optical networks," *J. Lightw. Technol.*, vol. 25, no. 1, pp. 67–74, Jan. 2007.

[2] W. Zhang, J. Sun, J. Wang, and L. Liu, "Multiwavelength mode-locked fiber-ring laser based on reflective semiconductor optical amplifiers," *IEEE Photon. Technol. Lett.*, vol. 19, no. 19, pp. 1418–1420, Oct. 1, 2007.

[3] L. Q. Guo and M. J. Connelly, "A novel approach to all-optical wavelength conversion by utilizing a reflective semiconductor optical amplifier in a co-propagation scheme," *Opt. Commun.*, vol. 281, no. 17, pp. 4470–4473, Sep. 2008.

[4] C. Michie, A. E. Kelly, J. McGeough, I. Armstrong, and I. Andonovic, "Polarization-insensitive SOAs using strained bulk active regions," *J. Lightw. Technol.*, vol. 24, no. 11, pp. 3920–3927, Nov. 2006.

[5] M. J. Connelly, "Wide-band steady-state numerical model and parameter extraction of a tensile-strained bulk semiconductor optical amplifier," *IEEE J. Quantum Electron.*, vol. 43, no. 1, pp. 47–56, Jan. 2007.

[6] J. W. D. Chi, L. Chao, and M. K. Rao, "Time-domain large-signal investigation on nonlinear interactions between an optical pulse and semiconductor waveguides," *IEEE J. Quantum Electron.*, vol. 37, no. 10, pp. 1329–1336, Oct. 2001.

[7] F. Devaux, Y. Sorel, and J. F. Kerdiles, "Simple measurement of fiber dispersion and of chirp parameter of intensity modulated light emitter," *J. Lightw. Technol.*, vol. 11, no. 12, pp. 1937–1940, Dec. 1993.

[8] M. J. Connelly, "Theoretical calculations of the carrier induced refractive index change in tensile-strained InGaAsP for use in 1550 nm semiconductor optical amplifiers," *Appl. Phys. Lett.*, vol. 93, no. 18, pp. 181111-1–181111-3, Nov. 2008.